European Polymer Journal 79 (2016) 163–175

Contents lists available at ScienceDirect

European Polymer Journal

journal homepage: www.elsevier.com/locate/europolj

Macromolecular Nanotechnology

Facile preparation of silver-based nanocomposites via thiol-methacrylate 'click' photopolymerization

Silvana V. Asmussen, Claudia I. Vallo *

Institute of Materials Science and Technology (INTEMA), University of Mar del Plata, CONICET, Juan B Justo 4302, 7600 Mar del Plata, Argentina

ARTICLE INFO

Article history:
Received 16 March 2016
Received in revised form 21 April 2016
Accepted 25 April 2016
Available online 27 April 2016

Keywords:
Thiol-ene
Photopolymerization
Silver NPs
Nanocomposites

ABSTRACT

Dispersions of silver nanoparticles (Ag NPs) in a tetrafunctional thiol were prepared by *in situ* reduction of silver nitrate with 2,6-di-*tert*-butyl-*para*-cresol. The obtained Ag NPs, were maintained in a stable colloidal state for more than eleven months at ambient temperature. The thiol monomer acts as both stabilizing agent and reactive solvent. Mixtures of dispersions of Ag NPs in thiol and a bifunctional methacrylate monomer were photoactivated with 2,2-Dimethoxy-2-phenylacetophenone (DMPA) or Camphorquinone (CQ) and then photopolymerized by irradiation with UV or visible light respectively. Dispersions containing high amounts of Ag NPs were more efficiently photopolymerized with the pair CQ/visible light. This is attributed to fact that the emission range of the UV LED (365 ± 5 nm) was overlapped with the surface plasmon resonance band of the Ag NPs ($\lambda < 400$ nm). Conversely, there was no overlap between the surface plasmon resonance band of the Ag NPs and the emission range of the visible LED (peak at 470 nm). Consequently, most of the visible light was absorbed by CQ, while a fraction of the UV light was absorbed by the Ag NPs and was not available for the photoinitiation process. The thiol-methacrylate matrix of the nanocomposites was characterized by measuring the glass transition temperature, the flexural modulus and the compressive strength. The low toxicity of the reactants used in the synthesis in combination with antimicrobial activity of Ag NPs makes the nanocomposite materials synthesized in this study very attractive for the preparation of biomaterials and coating with improved biocompatibility.

1. Introduction

Recently, organic-inorganic nanocomposite materials containing silver nanoparticles (Ag NPs) have attracted much attention due to their potential applications in a variety of fields such as optics, electronics, antimicrobial agents and conducting materials [1]. Typically, *in-situ* and ex-situ methods are the two main synthetic routes that lead to silver-polymer nanocomposites. The ex-situ method consists in dispersing dry silver nanoparticles produced beforehand by an appropriated chemical process into a polymer medium [2]. In the *in-situ* method, metal nanoparticles are generated directly in the matrix through chemical reduction of a precursor previously dissolved in the bulk [3,4]. Photochemical reduction by irradiating a dye sensitizer in the presence of silver ions also provides a convenient way to produce embedded nanoparticles in a polymer matrix [5,6]. An important feature in the preparation of polymeric materials containing noble metal nanoparticles is the need to keep the particles physically isolated, in order to prevent irreversible aggregation. The stability of the Ag NPs is commonly

* Corresponding author.
E-mail address: civallo@fi.mdp.edu.ar (C.I. Vallo).

http://dx.doi.org/10.1016/j.eurpolymj.2016.04.035
0014-3057/

achieved using different capping molecules, which bind onto their surface, avoiding their aggregation. Adsorption of organothiol molecules on silver surfaces has been widely used to fabricate self-assembled monolayers or modify surface properties in a broad range of novel technological applications [7–10].

The present study describes a simple method for preparing stable silver nanoparticles (Ag NPs) in a tetrafunctional thiol monomer. The dispersions of Ag NPs in tetrafunctional thiol were mixed with stoichiometric amounts of a bifunctional methacrylate monomer. Thiol-ene systems modified with different amounts of Ag NPs were photoactivated with 2,2-Dimethoxy-2-phenylacetophenone or Camphorquinone and then photopolymerized by irradiation with UV or visible light respectively. Characterization of the thiol-methacrylate network was carried out by measuring the glass transition temperature, the flexural modulus and the compressive strength. To the best of our knowledge, this is the first report describing the *in situ* synthesis of Ag NPs using a thiol monomer as both stabilizing agent and reactive solvent.

2. Experimental

2.1. Materials

Silver nitrate ($AgNO_3$, ⩾99%,), Pentaerythritol tetra(3-mercaptopropionate) (PETMP, >95%), 2,2-Dimethoxy-2-phenylacetophenone (DMPA, 99%), Camphorquinone (CQ, 99%) and 2,6-di-*tert*-butyl-*p*-cresol (BHT) were from Sigma Aldrich, USA. The methacrylate resin was 2,2-bis[4-(2-methacryloxyethoxy) phenyl]propane (BisEMA, 98%, from Esstech, Essington, PA). Absolute ethanol was from Merck, USA. The resins were activated for UV or visible light polymerization by the addition of 1 wt% DMPA or 1 wt% CQ respectively. The UV light source was assembled from a light-emitting diode (LED) with its irradiance centered at 365 nm (OTLH-0480-UV, Optotech). The intensity of the LED was 175 mW/cm^2. The visible light source was a LED unit (VALO, Ultradent, USA) with its irradiance centered at 470 nm and light intensity of 600 mW/cm^2. The structure of the monomers and photoinitiators is shown in Scheme 1.

2.2. Preparation of dispersions of Ag NPs

Colloidal dispersions of silver particles were obtained by reduction of silver nitrate in Pentaerythritol tetra(3-mercaptopropionate) (PETMP) by a two-phase liquid-liquid method [11]. First, 0.0632 g $AgNO_3$ were dissolved in 4 g absolute ethanol (Solution A). The solution was stirred at room temperature until complete dissolution of the $AgNO_3$ was achieved. Then 0.1, 0.2, 0.25 and 0.5 g of Solution A were mixed with 1 g of PETMP containing 1000 ppm BHT in order to prepare dispersions having 1000, 2000, 2500 and 5000 ppm of Ag NPs in PETMP. Dispersions containing lower amounts of Ag were prepared from 0.1 g Solution A and the required amount of PETMP. The two-phase mixture was vigorously stirred. The reaction was carried out in glass tubes placed in a thermostat held at 70 °C allowing continuous evaporation of volatiles. The reaction was allowed to proceed for ~24 h in order to ensure complete evaporation of the ethanol. Silver cations were reduced by the BHT present in PETMP. Mixtures thiol-methacrylate were prepared by mixing the PETMP containing Ag NPs with stoichiometric amounts of BisEMA. The stoichiometry of functional groups for total thiol (—SH) and ene (—C=C) was 2:1. The silver proportion in mixtures PETMP-BisEMA was varied in the range: 200–2500 ppm. Scheme 2 is a schematic diagram of the synthesis of Ag NPs in thiol followed by the preparation of nanocomposites by photopolymerization.

2.3. Photopolymerization

Measurements of conversion of methacrylate groups versus irradiation time were carried out at room temperature (20 °C) using near infrared spectroscopy (NIR) with a Nicolet 6700 Thermo Scientific. The NIR spectra were acquired over the range 4500–7000 cm^{-1} from 16 co-added scans at 2 cm^{-1} resolution. The resins were contained in a 10 mm diameter well constructed from a rubber gasket material sandwiched between two glass plates. The thickness of the samples was 2 mm. With the assembly positioned in a vertical position, the light source was placed in contact with the glass surface. The samples were irradiated at regular time intervals and the spectra were collected immediately after each exposure interval. These spectra were corrected with the background spectrum collected through an empty mould assembly fitted with only one glass slide to avoid internal reflectance patterns. The conversion of methacrylate groups was calculated from the decay of the absorption band located at 6165 cm^{-1}. Two replicates were used in the measurement of conversion. The peak corresponding to the S—H stretch of the thiol is located at 2568 cm^{-1} in the mid-IR region, however thiol absorbance was below detectable limits for the formulation studied. Thus, the conversion of thiol groups was measured by Raman spectroscopy. These studies were performed at room temperature (20 °C) with an Invia Reflex confocal Raman microprobe (Renishaw). A non-contact sampling objective (0.75 NA) with a 0.37 mm working distance was used and the excitation source was provided with the 785 nm emission line of a diode laser to the sample, thereby inducing the Raman scattering effect. The power of the laser was reduced to 10% to prevent damage by heating. At this power level, no thermal damage was observed. Raman spectra were taken averaging two acquisitions. The exposure time for each spectrum was 10 s. The spectra were collected in a Raman shift range between 400 and 1800 cm^{-1} at a spectral resolution of 4 cm^{-1}. The irradiated spot on the sample surface was focused to a diameter of ~2 mm. Samples were sandwiched between a slide and a cover slip separated by a 1.5 mm thick rubber spacer with a 10 mm diameter circular hole. The circular hole of the assembly was filled with

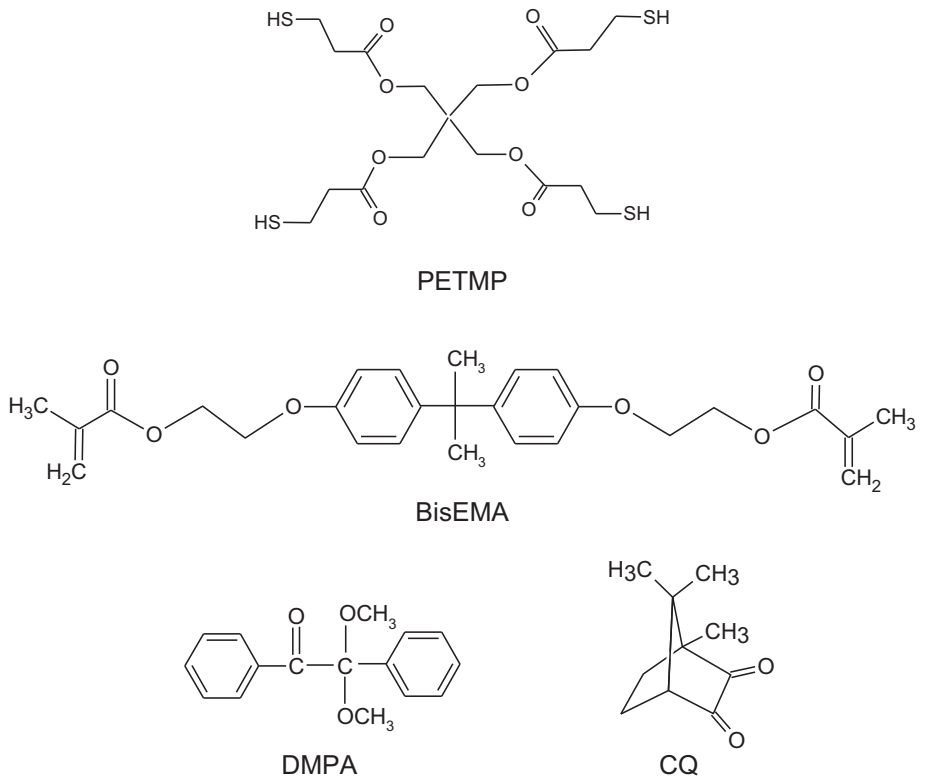

Scheme 1. Structure of the monomers and photoinitiators used in this study.

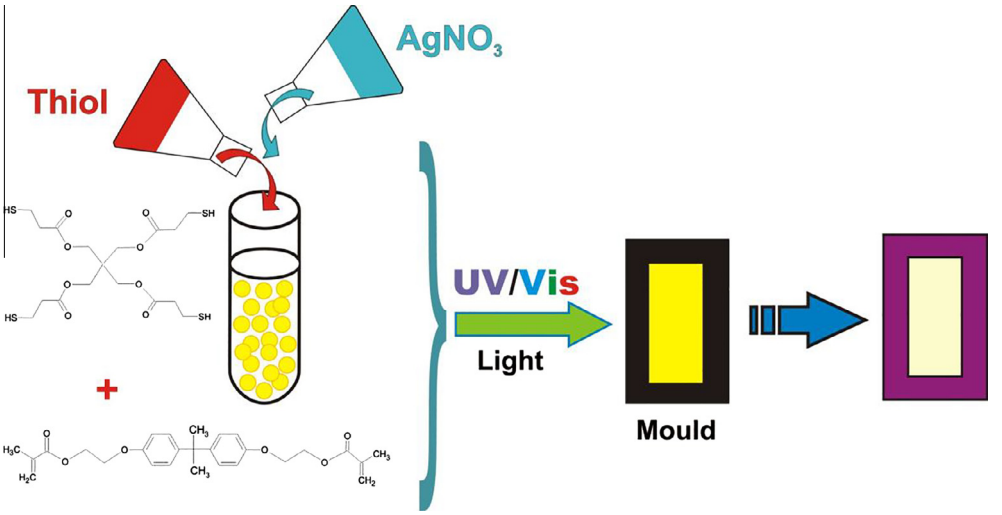

Scheme 2. Colloidal dispersions of Ag NPs in a tetrafunctional thiol obtained by reduction of silver nitrate by BHT. Nanocomposites were prepared by photopolymerization of mixtures of thiol containing Ag and a methacrylate monomer.

the reactive mixture and held using small clamps. Then, the assembly was introduced into the compartment of the Raman spectrometer for spectra collection. All spectra were collected at 300 mm below the surface of the coverslip. Samples were irradiated at consecutive irradiation intervals of 4 s. After each exposure interval, the samples were transferred to the Raman sample compartment for the spectrum collection. The conversion profiles were calculated from the decay of the characteristic absorption band of each reactive group. The conversion of methacrylate C=C double bonds was followed by the decay of

the band located at 1642 cm^{-1}, associated with the C═C stretching vibrations. The conversion of S—H group was assessed by the decay of the band at 2575 cm^{-1}. Two replicates of each of the resins were used in the measurement of conversion.

2.4. Characterization

The absorption spectra of dispersions of silver nanoparticles were measured with an UV–vis spectrophotometer 1601 PC Shimadzu at room temperature (20 ± 2 °C). The resins were contained in thin cells (~0.5 mm) constructed from two quartz microscope slides separated by a PTFE gasket. An identical cell containing the PETMP or PETMP-BisEMA monomers was used as the reference.

Observations to examine the morphology of the thiol-methacrylate materials containing Ag NPs were carried out with a JEOL 100 CX II transmission electron microscope (TEM) instrument operated at an accelerating voltage of 100 kV. Samples were sectioned using an LKB ultramicrotome with a diamond knife.

Dynamic mechanical thermal analysis (DMTA) tests in torsion deformation mode were performed from −70 °C to 120 °C using the Rheometer MCR 301 (Anton Paar GmbH) equipped with fixture for rectangular bars (SRF92) and a temperature chamber (CTD600). Rectangular specimens with dimensions (ca. 40 ± 0.5 mm × 10 ± 0.05 mm × 1.5 ± 0.05 mm) (length × width × thickness) were tested. The frequency of oscillations was fixed at 1 Hz and the heating rate was of 5 °C/min. Previously, a strain sweep test in a representative sample was performed at 20 °C and 1 Hz in order to determine the linear viscoelastic range and select a strain value to apply in temperature sweeps. The selected strain value was 0.05%. A small axial force (around −0.5 N) was applied in all test specimens in order to maintain a net tension.

Flexural and compressive tests were carried out at room temperature with an Instron testing machine (model 4467) at a crosshead displacement rate of 1 mm/min. The flexural modulus, E was measured in three-point bending using sample dimensions recommended by the ISO 4049:2000(E): (25 ± 2) mm × (3 ± 0.1) mm × (2.5 ± 0.1) mm. Results were computed using the standard formula:

$$E = \frac{L^3 P}{4bd^3 y}$$

where L is the length between the supports (16 mm), P is the load, b is the width of the specimen, d is the thickness of the specimen, and y is the deflection at the center. The results are the average of five measurements.

PETMP-BisEMA networks were also tested under uniaxial compression. Samples for compression testing were made by injecting the resins into polypropylene cylindrical disposable molds of 6 mm internal diameter (D). Samples were irradiated for 120 s on each side. After removal from the molds, the compression specimens were machined to reach their final dimensions. Cylindrical specimens having an aspect ratio L/D of 1.5 were deformed between metallic plates lubricated with molybdenum disulfide. The deformation was calculated directly from the crosshead speed. True stress-deformation curves were obtained by dividing the load by the cross-sectional area. The yield stress was determined at the maximum load. All test specimens were photopolymerized in ambient at room temperature (20 ± 2 °C). A set of test specimens was also post-cured at 100 °C for 2 h. The results are the average of five measurements.

3. Results and discussion

This section is divided into four parts concerned first with the synthesis and characterization of silver nanoparticles in a tetrafunctional thiol monomer, followed by studies of photopolymerization of a thiol-methacrylate network containing different amounts of silver nanoparticles. The last two sections show results of thermal and selected mechanical properties of the thiol-methacrylate network in which the silver nanoparticles were dispersed.

3.1. Synthesis and characterization of dispersions of Ag NPs in thiol monomer

Ag NPs were *in situ* synthesized in PETMP thiol monomer through reduction of $AgNO_3$ with BHT using a one-step synthesis method. Reagents commonly used to reduce silver ions in the preparation of Ag/polymer nanocomposites include N,N-dimethylformamide, hydrazine, ferric ions, and sodium borohydride. Unfortunately, those reducing agents exhibit undesired toxicity, which limit their application in packaging and medical products. Kassaee et al. [3] proposed that silver ions can be reduced by BHT. Application of heat or light dissociates the O—H bond of BHT rendering very stable oxygen radicals. The authors found that hydrogen radicals ($H^{\cdot}$) generated from thermolysis of BHT could reduce silver ions leading to formation of Ag NPs. BHT is an antioxidant phenolic acid that is often added to foods to preserve fats and is also used as an antioxidant additive in polymers. In addition, BHT is added to formulations of light-cured dental composite as inhibitor to prevent premature polymerization during storage. Thus, BHT is an attractive reducing agent for applications that demand low toxicity.

Fig. 1 is a picture of dispersions of Ag NPs in PETMP. The dispersions showed a pale yellow[1] color, which became greenish yellow with increasing concentration of Ag NPs.

[1] For interpretation of color in Fig. 1, the reader is referred to the web version of this article.

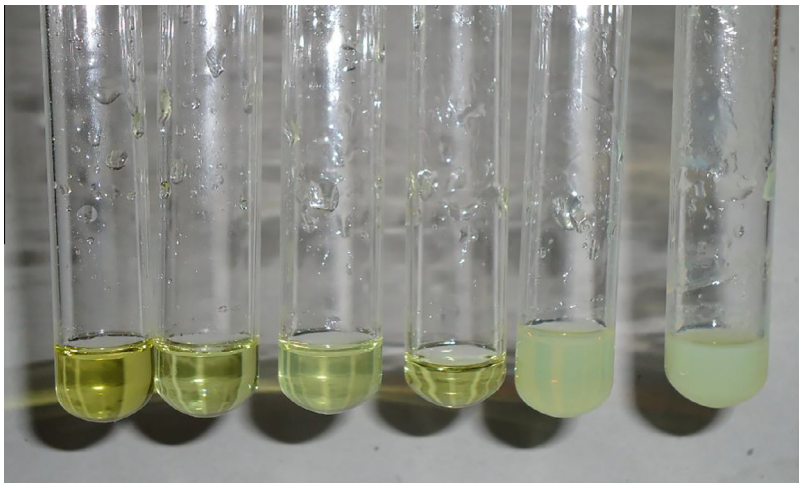

Fig. 1. Dispersions of Ag NPs in PETMP (200, 1000, 1500, 2000, 2500 and 5000 ppm) taken 24 h after the synthesis.

No appreciable change in color occurred after 11 months of storage in air at room temperature. The dispersions of Ag NPs in PETMP were examined by UV–vis spectroscopy. Fig. 2a shows the absorption spectra of a dispersion of Ag NPs in PETMP. The absorption spectra of Ag NPs (5–10 nm in diameter) prepared in the BisEMA monomer [4] is also shown in Fig. 2a for comparison. Fig. 2b illustrates UV–vis spectra of dispersions containing 1000 and 2500 ppm of Ag NPs in PETMP.

The Ag NPs in PETMP show well-defined surface plasmon resonance absorption in the UV region ($\lambda < 400$ nm). UV–vis spectra in Figs. 2a and 2b were taken from thin films in order to ensure the validity of Beer-Lambert law. The absorbance values of thin films at wavelengths higher than 450 nm are comparatively low, however, they are not zero and, consequently, the suspensions shown in Fig. 1 display a pale color. After storage in air and in the dark for 11 months the silver sols were still clear, and no appreciable change in the UV–vis spectra obtained after this storage period was observed. Since the reduction was performed in air it has to be expected that the silver nanoparticles are partially oxidized, due to the sensitivity of the colloidal silver nanoparticles toward oxidation [12]. Henglein has shown that such oxidation processes are associated with a strong decrease and broadening of the absorption bands [12]. The negligible changes of the absorption bands observed after 11 months of storage demonstrate that PETMP is an efficient protective agent, which prevents particle coalescence and enables long term stability. Battocchio et al. studied the local chemistry and chemical structure of silver nanoparticles stabilized with the organic thiol allylmercaptane [9]. The authors demonstrated that the Ag NPs structure is described by a core shell morphology resulting in metallic Ag cores surrounded by Ag_2S-like shell. An external layer of thiol molecules is grafted to the Ag NPs surface through Ag—S chemical bonds. In a recent report, Zhang et al. studied the adsorption of reactive aromatic organothiol onto silver nanoparticles in water [10]. The authors presented further confirmation of the Ag NPs core–shell formation.

According to Mie's theory, the resonance position and shape are closely related to the particle size and shape [13]. Fig. 2b indicates a broadening of the UV–vis spectra with increasing content of Ag NPs. This observation is in agreement with results reported by Battocchio et al. [9], who observed that by increasing the Ag/thiol mass ratio, larger Ag NPs were obtained. The increase in particle size with increasing amounts of Ag is attributed to a reduction in the PETMP/Ag mass ratio. When the amount of thiol monomer is not enough, a complete protection layer cannot be formed giving as a result agglomeration of metal clusters. As particle size continues to increase most visible wavelengths are reflected, giving the nanoparticles clear or translucent color (Fig. 1 samples 5–6). The shift of the absorption bands from UV–vis studies (Fig. 2a) indicates that the Ag NPs prepared in PETMP were smaller than those prepared in BisEMA. [13] The UV–vis absorption spectrum of a dispersion of Ag NPs in a mixture PETMP-BisEMA 1:2 mol ratio is shown in Fig. 2a. It is seen a broadening of the absorption spectra compared with those of dispersions of Ag NPs in PETMP. The surface plasmon resonance absorption of the Ag NPs in the mixture thiol-methacrylate starts in the visible region ($\lambda \sim 450$ nm) indicating a change in the morphology of the nanoparticles. This difference in size of Ag NPs prepared in different monomers can be attributed to a stronger interaction of PETMP with the Ag NPs compared with BisEMA. This trend is in agreement with results reported by Sigoli et al. on the preparation of Ag NPs in N,N-dimethylformamide and N,N-dimethylacetamide [14].The comparatively smaller average size of nanoparticles obtained using N,N-dimethylacetamide was correlated to a stronger interaction of silver ions/N,N-dimethylacetamide compared to that of silver ions/N,N-dimethylformamide.

Morphological information on Ag NPs in PETMP-BisEMA network was obtained from TEM images.

TEM micrographs presented in Fig. 3a–d reveal the presence of Ag NPs distributed in the polymer network and the formation of aggregated nanoparticles is also recognized. The presence of aggregates is attributed to a reduction in the PETMP/Ag NPs mass ratio in the preparation of dispersions of Ag NPs in PETMP-BisEMA by adding BisEMA to dispersions

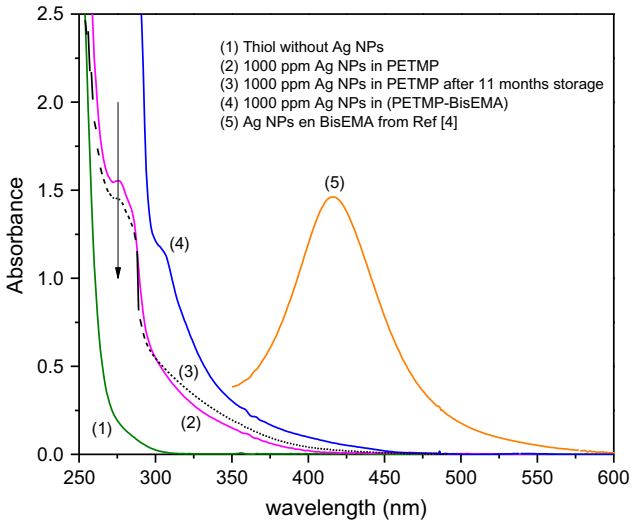

Fig. 2a. UV–vis spectra of dispersions of Ag NPs in PETMP, BisEMA from Ref. [4], and a mixture PETMP-BisEMA 1:2 mol ratio.

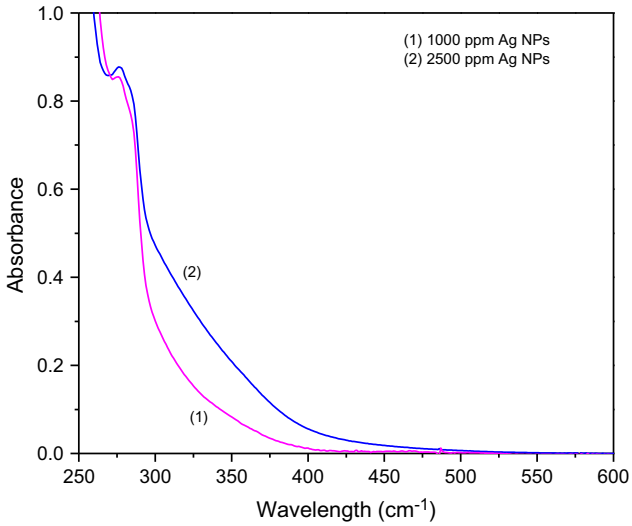

Fig. 2b. UV–vis spectra of dispersions containing different amounts of Ag NPs in PETMP.

of Ag NPs in PETMP. When the amount of thiol monomer is reduced, in some regions the protection layer is disrupted and, therefore, the particles form aggregates.

In a previous report, we showed that at silver mass fractions lower than 300 ppm BisEMA acts as an efficient particle stabilizer preventing particle coalescence, whereas at silver concentration above that value, precipitation on the walls of the container occurred within days after the preparation of the solutions [4]. Results presented show that up to 2500 ppm Ag NPs can be dispersed in mixtures PETMP-BisEMA.

3.2. Photopolymerization

In this section, the photopolymerization of mixtures thiol-methacrylate containing different amounts of Ag NPs is described. Dispersions of Ag NPs in PETMP-BisEMA were photoactivated with 1 wt% of DMPA or 1 wt% of CQ. Mixtures containing DMPA were photo polymerized with a 365-nm LED, while mixtures containing CQ were photo polymerized with a 470-nm LED. The conversion of C=C were calculated by NIR spectroscopy from the decay of the absorption band located at 6165 cm^{-1}. It is worth mentioning that the absorption band of the —SH group in the Mid-IR range (2572 cm^{-1}) had very low intensity; therefore, the conversion of thiol groups was measured by Raman spectroscopy. Fig. 4 shows representative spectra of a mixture thiol-methacrylate 1:2 mol ratio. The band located at 1642 cm^{-1} is associated with the C=C stretching

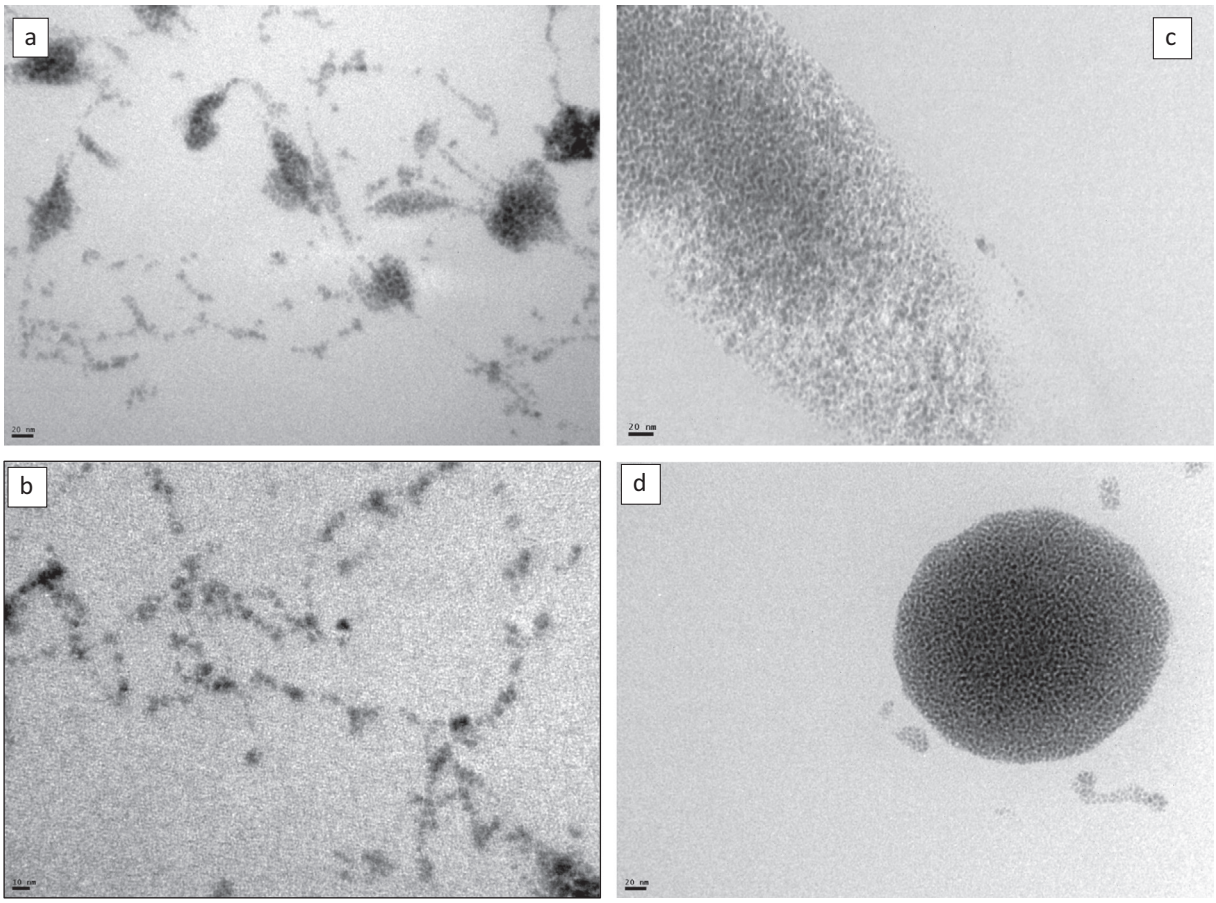

Fig. 3. TEM images of 500 ppm Ag NPs dispersed in PETMP-BisEMA. (a) The length of the bar is equivalent to 20 nm. (b) The length of the bar is equivalent to 10 nm. (c) and (d) TEM pictures showing agglomerations of Ag NPs in a dispersion of 2500 ppm Ag NPs in PETMP-BisEMA. The presence of agglomerates in figs. (c) and (d) is considered responsible for the translucent effect of sample (5) in Fig. 1.

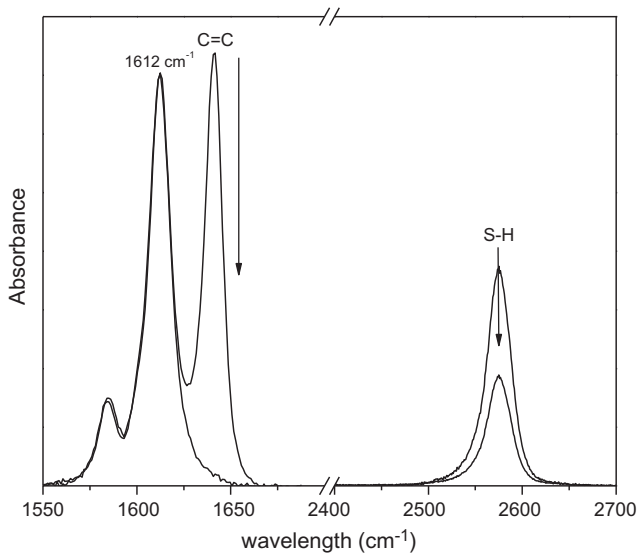

Fig. 4. Characteristic peaks in Raman spectra of the thiol/methacrylate (PTEMP/BisEMA) mixture. The band representing the methacrylate double bond is located at 1642 cm^{-1}. The band at 2575 cm^{-1} is assigned to the S—H group. The band at 1612 cm^{-1}, was selected as internal reference band.

vibrations. The band at 1612 cm^{-1}, which characterizes the aromatic ring, was selected as internal reference band. The conversion of thiol groups was calculated from the decay of the band located at 2575 cm^{-1} associated with the S—H stretching vibrations. Figs. 5 and 6 show the conversion of C=C in PETMP-BisEMA mixtures containing different amounts of Ag NPs, photoactivated with DMPA and CQ respectively.

Thiol-ene systems polymerize by a free-radical chain mechanism involving two steps: an initial addition of the thiyl radical to the carbon of an -ene functionality and a subsequent hydrogen abstraction of a thiol group by a carbon-centered radical to give a thiyl radical [15–17]. Termination occurs by radical-radical coupling. Initiation of thiol-ene photopolymerization can be carried out by either the excitation of an aryl aliphatic ketone followed by α-bond cleavage, or the excitation of a ketone followed by hydrogen transfer [15–17]. The excitation of DMPA under irradiation at 365 nm gives benzoyl and dimethoxybenzyl radicals. A rearrangement of the dimethoxybenzyl radical produces a methyl radical and methyl benzoate. The methyl and benzoyl radicals may insert into a C=C bond directly or abstract a hydrogen from a thiol group. In either case, the two-step process characteristic of the thiol-ene free-radical chain reaction is initiated as shown in Scheme 3.

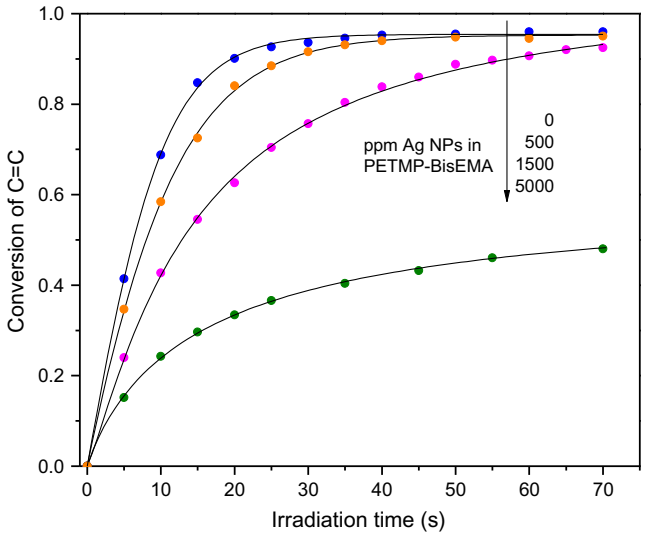

Fig. 5. Conversion of methacrylate groups versus irradiation time in PETMP-BisEMA containing different amounts of Ag NPs (ppm). Samples containing 1 wt% DMPA were irradiated at 365 nm. The specimens were 10-mm diameter and 2-mm thick.

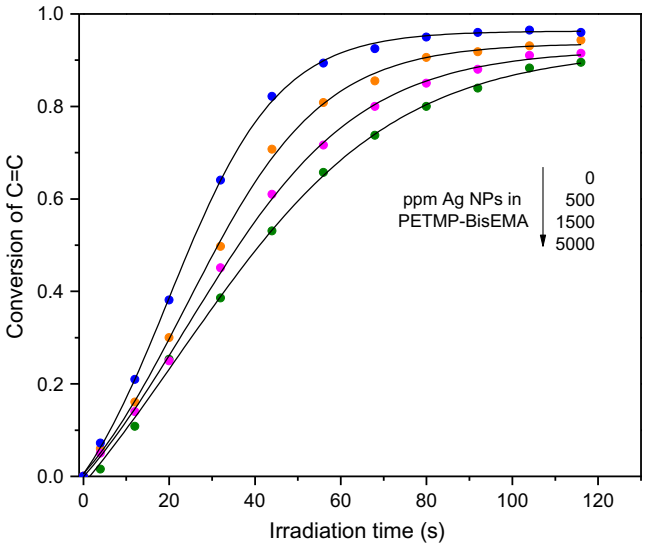

Fig. 6. Conversion of methacrylate groups versus irradiation time in PETMP-BisEMA containing different amounts of Ag NPs (ppm). Samples containing 1 wt% CQ were irradiated at 470 nm. The specimens were 10-mm diameter and 2-mm thick.

Alternatively, CQ is excited under visible light irradiation (λ = 470 nm), to the excited singlet state which converts to the reactive triplet state CQ* via an efficient intersystem crossing. CQ* can react with hydrogen donors to generate radicals by proton transfer to give pinicol and radicals derived from the hydrogen donor [18,19]. Fig. 6 shows that CQ is an efficient photoinitiator of the thiol-methacrylate system studied in this research. This confirms that there is an efficient hydrogen transfer from the PETMP to the excited triplet state of CQ, to give thiyl radicals and semipinacol radicals. The consumption of the S—H groups was assessed by Raman spectroscopy (Fig. 4). While the methacrylate groups were totally consumed after few seconds of irradiation, about 40% of thiol groups remained unreacted. This is attributed to homopolymerization of the methacrylate monomer.

Concerning the thiol-ene systems modified with Ag NPs, It is seen in Figs. 5 and 6 that as the Ag NPs concentration increased it became more difficult to cure the specimens. Although the final conversions in resins containing 0 or 1500 ppm Ag NPs were similar, the polymerization rate decreased appreciably on increasing the Ag NPs concentration. When an assembly of nanoparticles is irradiated by a plane wave, the incident light is scattered and absorbed by each particle to a certain extent [20]. As a result of these absorption and scattering processes the transmitted light decreases along the propagation direction of the incident light. The UV–vis spectra of the photoinitiators DMPA and CQ, a dispersion of Ag NPs in PETMP-BisEMA, and the wavelengths of the emitted light from the UV and visible LEDs are presented in Fig. 7.

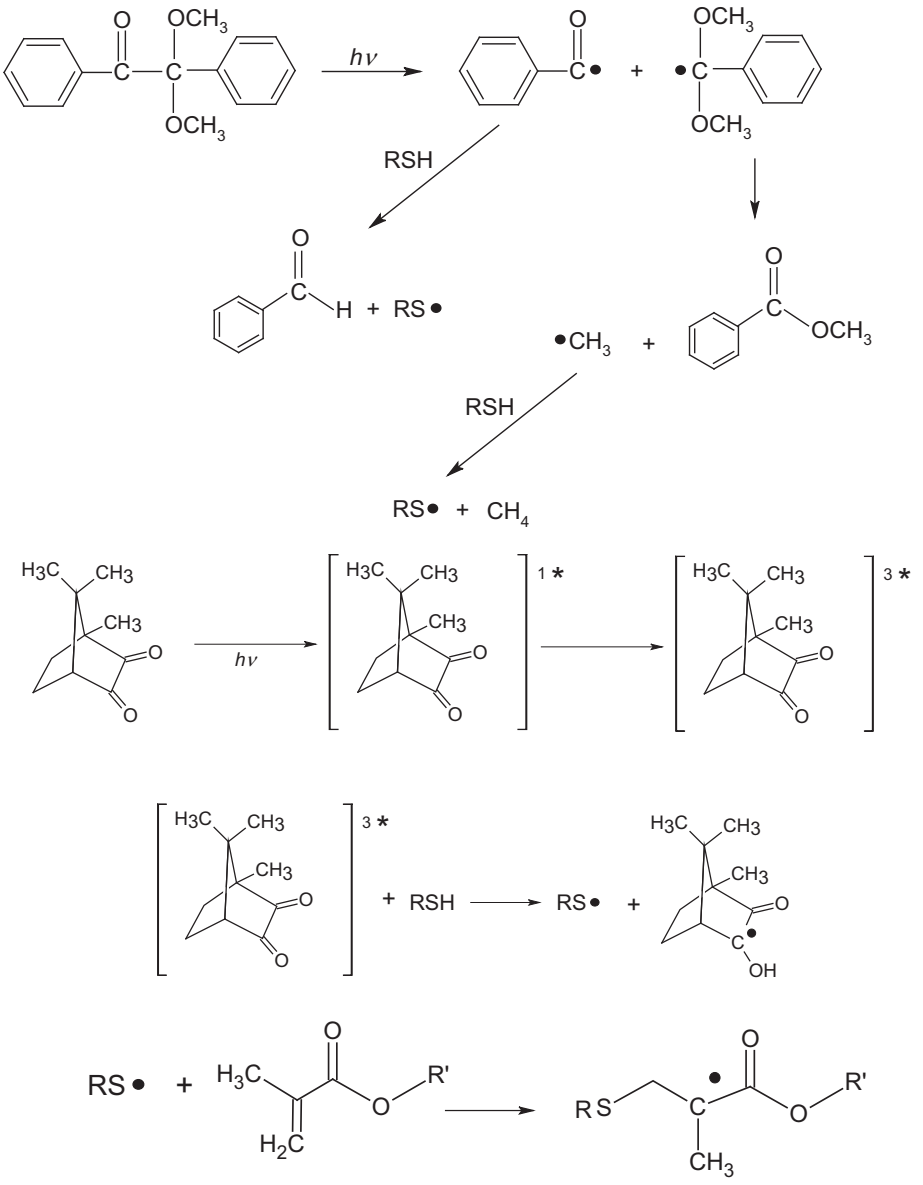

Scheme 3. Photolysis of (a) DMPA and (b) CQ under irradiation to produce initiating species for the polymerization of thiol-methacrylate.

It is seen that the UV LED source emits in a narrow wavelength centered at 365 nm while the Ag NPs absorb light in the range 350–550 nm. Thus, a fraction of the incident light is absorbed by the Ag NPs. The presence of light absorbing species in a photo curing resin inevitably results in attenuation of the light intensity along the radiation path. The reduced polymerization rate with increasing Ag NPs content is attributed to the related losses which increase with the Ag NPs content [20]. Fig. 6 shows that the reduced conversion with increasing amounts of Ag NPs in resins photoactivated with CQ is much less marked compared with those photoactivated with DMPA (Fig. 5). This is attributed to a lower overlap of the spectral emission of the 470-nm LED with the surface plasmon resonance absorption band of the Ag NPs (Fig. 7). From these observations, it is clear that in order to cure layers of resins containing high proportions of Ag NPs, the light source-photoinitiator pair must be carefully selected.

Previous reports have shown that if benzophenone or some other diarylketone is used to initiate thiol-ene polymerization, most of the diarylketone remains unconsumed at the end of the polymerization and remains in the film as a plasticizer and photoreactive species [15]. This can severely hinder the long-term color stability (yellowing) of films exposed to sunlight or even certain types of room light. One way of avoid this problem is to use an N-substituted maleimide, which abstracts a hydrogen from the labile thiol group. Because maleimides are quite reactive, they are consumed by the radical chain process that they initiate and hence do not remain in the film after exposure. Alternatively, those problems can be circumvented by using CQ as photoinitiator of the thiol-ene polymerization. CQ displays an intense dark yellow color due to the presence of the conjugated diketone chromophore that absorbs at 470 nm (Fig. 7). During irradiation of CQ and reduction of one of the carbonyl groups, the conjugation is destroyed, causing loss of the yellow color. This is illustrated in Fig. 8, which shows a continuous decrease in absorbance with irradiation time.

By irradiating a 3-mm thick sample for 130 s the absorbance of the CQ in the sample was reduced to 25% of the initial value. For a thick-section cure, it is advantageous to use photobleaching initiators in which light absorption by the initiator photoproducts is lower than that by the original photoinitiator molecule, thereby allowing more light to pass through the system [21]. Fig. 8 shows that the photolysis products of CQ in PETMP-BisEMA are transparent at the irradiating wavelengths, consequently the consumption of the CQ leads to an increase in light intensity in the underlying lays. The clean and rapid photobleaching of CQ in PETMP-BisEMA makes it very attractive for polymerization of thick sections. Photopolymerization of methacrylate and epoxy resins upon irradiation with visible light is commonly photoinitiated by the pair camphorquinone (CQ)/amine [21–23]. Unfortunately, amines have intrinsic disadvantages such as odor, toxicity, and migration in UV-curing technology. An issue of primary concern in packaging systems is that the low molecular weight species may migrate from the coating into a packaged product. Similarly, in light-cured dental restorative resins, research has been directed toward the synthesis of amines with improved biocompatibility [24]. Results obtained in this research show that thiol-methacrylate resins based on PETMP-BisEMA are efficiently polymerized with visible light by CQ in the absence of amine and thereby prevents the complications related to the use of amines. In addition, silver and silver ions have long been known to exhibit powerful antimicrobial activity [6,25,26]. In this study we found that Ag NPs can be prepared through reduction of $AgNO_3$ with a low toxicity reducer (BHT). This makes the light-cured PETMP-BisEMA containing Ag NPs very attractive for the preparation of biomaterials and coating with improved biocompatibility. In addition, the nanocomposites can be used for the production of filters for optical devices [27,28].

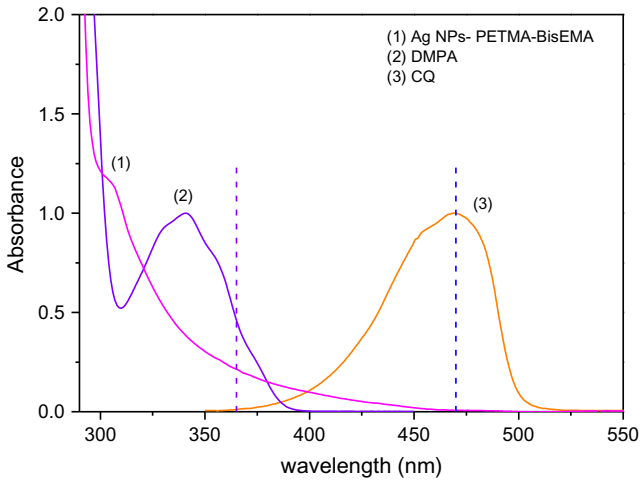

Fig. 7. UV–vis spectra of the photoinitiators DMPA and CQ, and resin PETMP-BisEMA containing Ag NPs. The dashed lines represent the wavelengths of the emitted light from the UV (365 nm) and visible (470 nm) LEDs.

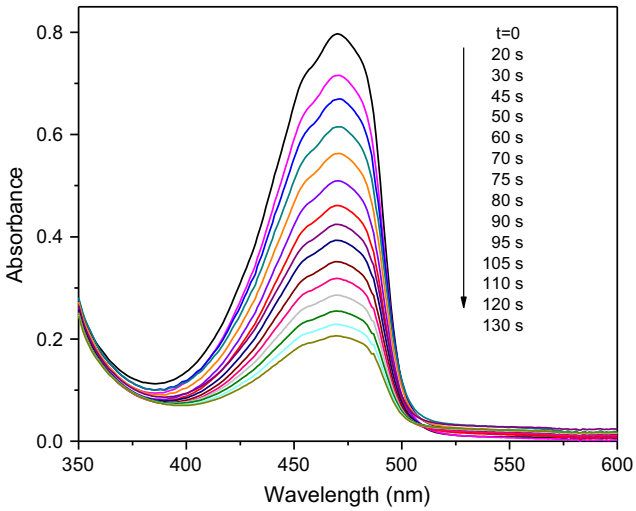

Fig. 8. Typical spectral changes during irradiation at 470 nm of a PETMP-BisEMA resin containing 1 wt% CQ. The specimen was 10-mm diameter and 3-mm thick.

3.3. DMTA studies

The glass transition temperature (Tg) is a critical polymer property because it often determines which applications a polymer is suitable for. Thus, the Tg of the thiol-ene network used as a matrix of the nanocomposites containing Ag NPs was assessed. Fig. 9 is a plot of tan δ and storage modulus versus temperature derived from dynamic mechanical thermal analysis (DMTA). One of the advantages of thiol-ene networks is their high network uniformity characterized in terms of the width of the glass transition region [29]. As thiol-ene networks are produced by a step-growth process, high molecular weights are not obtained until late in the reaction. As such, thiol-ene polymers typically form highly uniform networks, in terms of cross-link density, that possess narrow glass transition regions. This can be quantified by the full width at half-maximum for the tan δ in the transition region. The thiol-ene network based in PETMP-BisEMA exhibits a Tg half-height widths equal to 18 °C. This contrasts with a much broader glass transition extending over about 150 °C, typical of photocured multifunctional methacrylates [16]. The narrower tan δ plot in Fig. 9 for the film prepared from PETMP-BisEMA indicates a more uniform crosslink density. The effect of a post-curing treatment at 100 °C for 2 h on the Tg will be discussed in the next point (3.4 and Table 1).

3.4. Mechanical properties

Some selected mechanical properties were measured for further characterization of the PETMP-BisEMA network. Typical plots of load versus strain obtained from flexural tests and compressive strength versus deformation obtained from

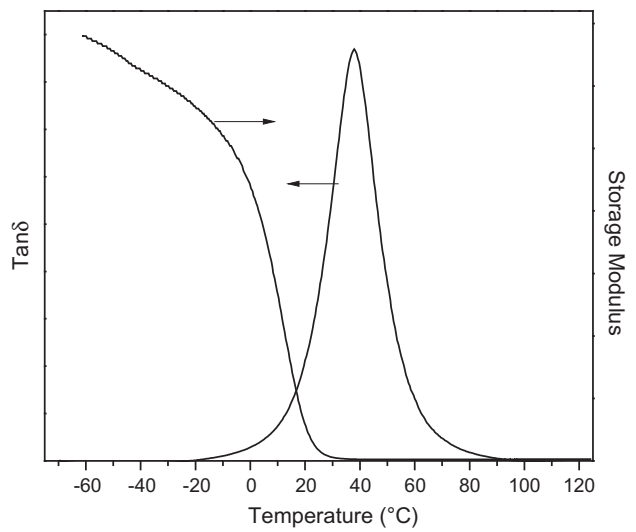

Fig. 9. Tan δ and storage modulus versus temperature for PETMP:BisEMA 1:2 mol ratio.

Table 1
Flexural modulus (E) and compressive yield strength (σy) and Tg of PETMP-BisEMA 1:2 mol ratio. PC, post-cured at 100 °C; NP, without post-curing treatment.

Treatment	E (GPa)	σy (MPa)	Tg
NP	1.10 (±0.15)	41 (±2)	38 °C (±1)
P	1.04 (±0.12)	38 (±4)	38 °C (±1)

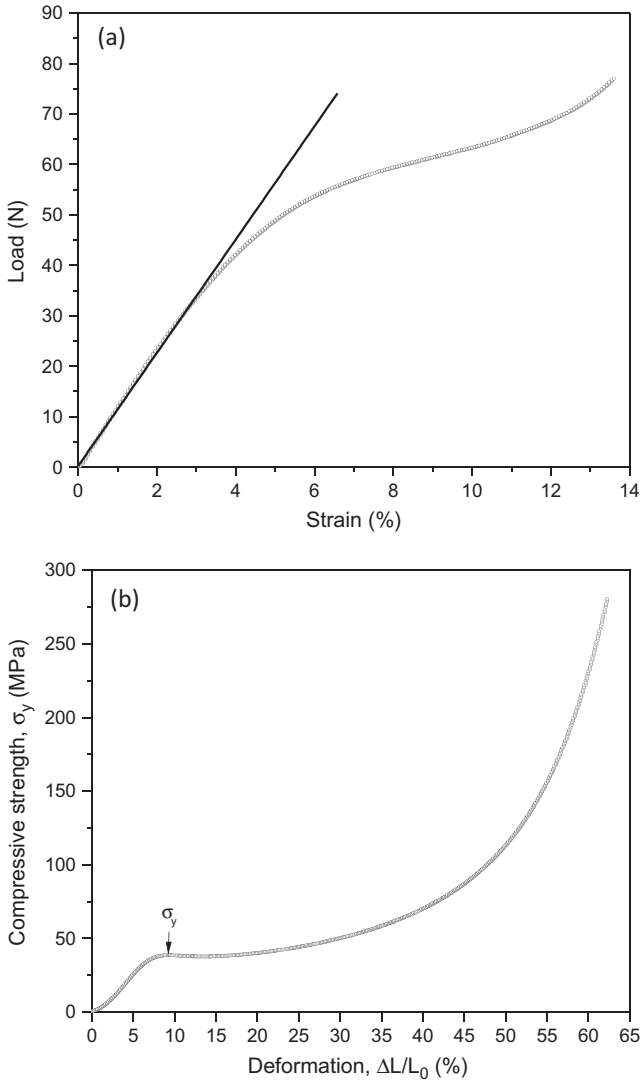

Fig. 10. (a) Typical plot of load versus strain obtained from flexural tests. (b) Typical plot of compressive strength versus deformation obtained from and compressive tests.

compressive tests are presented in Fig. 10(a) and (b) respectively. The values of the flexural modulus (E) and compressive strength (σy) are summarized in Table 1. It has been widely reported that the polymerization of dimethacrylates and epoxy resins in the absence of external heating leads to glassy resins in which only some of the available double bonds are reacted [30]. Before the completion of conversion, the vitrification phenomenon decelerates the reaction to a hardly perceptible rate, so that it may be impossible to achieve 100% conversion. The presence of non-reacted monomer can have a plasticizing effect on the polymer, thereby altering the physical and mechanical properties of the hardened material [30]. Post-curing treatments at ~20 °C above the Tg reduce the amount of non-reacted monomer, which results in increased flexural modulus and compressive strength [30]. In this study, a post-curing treatment at 100 °C for 2 h was performed in order to assess changes in the mechanical properties arisen from an incomplete cure of the PETMP-BisEMA network. Table 1 shows that

no significant increase in E, σy and Tg values resulted from the post-curing treatment. From this results it is concluded that the unreacted SH groups exists mainly as pendant chains instead of free leachable monomer.

4. Conclusion

Colloidal dispersions of silver nanoparticles (Ag NPs) in a tetrafunctional thiol can be prepared by *in situ* reduction of silver nitrate with 2,6-di-*tert*-butyl-*para*-cresol using a two-phase liquid-liquid method. The prepared dispersions of Ag NPs are maintained in a stable colloidal state for more than ten months at ambient temperature.

Mixtures of thiol containing Ag NPs and methacrylate monomer, photoactivated with DMPA or CQ, can be polymerized by irradiation with UV (365 nm) or visible (470 nm) light respectively. Dispersions containing higher amounts of Ag NPs are more efficiently photopolymerized with CQ because of the absence of overlap between the surface plasmon resonance band of the Ag NPs and the emission range of the visible LED.

The low toxicity of the reactants used in the synthesis in combination with antimicrobial activity of Ag NPs makes the materials synthesized in this study very attractive for the preparation of biomaterials and coating with improved biocompatibility.

Acknowledgements

The financial support provided by the ANPCyT (PICT-1008-2010) and CONICET is gratefully acknowledged.

References

[1] D. Pozo Perez (Ed.), Silver Nanoparticles, InTech, 2010 (ISBN: 978-953-307-028-5).
[2] C. Manz, L. Williams, R. Mohseni, E. Zlotnikov, A. Vasiliev, Dispersibility of organically coated silver nanoparticles in organic media, Colloids Surf. A: Physicochem. Eng. Aspects 385 (2011) 201.
[3] M.Z. Kassaee, M. Mohammadkhani, A. Akhavan, R. Mohammadi, In situ formation of silver nanoparticles in PMMA via reduction of silver ions by butylatedhydroxytoluene, Struct. Chem. 22 (2011) 11.
[4] S.V. Asmussen, C.I. Vallo, Synthesis of silver nanoparticles in surfactant-free light-cured methacrylate resins, Colloids Surf. A: Physicochem. Eng. Aspects 466 (2015) 115.
[5] Z. Yang, D. Zhai, X. Wang, J. Wei, In situ synthesis of highly monodispersednonaqueous small-sized silver nano-colloids and silver/polymer nanocompos-ites by ultraviolet photopolymerization, Colloids Surf. A: Physicochem. Eng. Aspects 448 (2014) 107.
[6] G. Colucci, E. Celasco, C. Mollea, F. Bosco, L. Conzatti, M. Sangermano, Hybrid coatings containing silver nanoparticles generated in situ in a thiol-ene photocurable system, Macromol. Mater. Eng. 296 (2011) 921.
[7] M. Oliveira, D. Ugarte, D. Zanchet, A. Zarbin, Influence of synthetic parameters on the size, structure, and stability of dodecanethiol-stabilized silver nanoparticles, J. Colloids Interf. Sci. 292 (2005) 429.
[8] H.S. Toh, C. Batchelor-McAuley, K. Tschulik, R.G. Compton, Chemical interactions between silver nanoparticles and thiols: a comparison of mercaptohexanol against cysteine, Sci. China Chem. 57 (2014) 1199.
[9] C. Battocchio, C. Meneghini, I. Fratoddi, I. Venditti, M.V. Russo, G. Aquilanti, C. Maurizio, F. Bondino, R. Matassa, M. Rossi, S. Mobilio, G. Polzonetti, Silver nanoparticles stabilized with thiols: a close look at the local chemistry and chemical structure, J. Phys. Chem. C 116 (2012) 19571.
[10] S.M. Ansar, G.S. Perera, P. Gomez, G. Salomon, E.S. Vasquez, I.W. Chu, S. Zou, C.U. Pittman, K.B. Walters, D. Zhang, Mechanistic study of continuous reactive aromatic organothiol adsorption onto silver nanoparticles, J. Phys. Chem. C 117 (2013) 27146.
[11] M. Brust, M. Walker, D. Bethell, D.J. Schiffrin, R. Whyman, Synthesis of thiol-derivatised gold nanoparticles in a two-phase liquid-liquid system, J. Chem. Soc., Chem. Commun. (1994) 801.
[12] A. Henglein, Colloidal silver nanoparticles: photochemical preparation and interaction with O_2, CCl_4, and some metal ions, Chem. Mater. 10 (1998) 444.
[13] K.L. Kelly, E. Coronado, L.L. Zhao, G. Schatz, The optical properties of metal nanoparticles: the influence of size, shape, and dielectric environment, J. Phys. Chem. B 107 (2003) 668.
[14] L.P. Costa, A.L. Formiga, I.O. Mazali, F.A. Sigoli, Spontaneous formation ofhighly dispersed spheroidal metallic silver nanoparticles in surfactant-free N, N-dimethylacetamide, Synth. Met. 161 (2011) 1517.
[15] C.E. Hoyle, T.Y. Lee, T. Roper, Thiol-enes: chemistry of the past with promise for the future, J. Polym. Sci. Part A Polym. Chem. 42 (2004) 5301.
[16] C.E. Hoyle, C.N. Bowman, Thiol-ene click chemistry, Angew. Chem. Int. Ed. 49 (2010) 1540.
[17] M.A. Tasdelen, B. Kiskan, Y. Yagci, Externally stimulated click reactions for macromolecular syntheses, Prog. Polym. Sci. 52 (2016) 19.
[18] M. Uygun, M.A. Tasdelen, Y. Yagci, Influence of type of initiation on thiol-ene "click" chemistry, Macromol. Chem. Phys. 211 (2010) 103.
[19] P. Xiao, F. Dumur, M. Frigoli, B. Graff, F. Morlet-Savary, G. Wantz, H. Bock, J.P. Fouassier, D. Gigmes, J. Lalevée, Perylene derivatives as photoinitiators in blue light sensitive cationic or radical curable films and panchromatic thiol-ene polymerizable films, Eur. Polym. J. 53 (2014) 215.
[20] M. Quinten, Optical Properties of Nanoparticle Systems, Wiley-VCH Verlag & Co. KGaA, Germany, 2011.
[21] S.V. Asmussen, G. Arenas, W.D. Cook, C.I. Vallo, Photoinitiation rate profiles during polymerization of a dimethacrylate-based resin photoinitiated with camphorquinone/amine influence of initiator photobleaching rate, Eur. Polym. J. 45 (2009) 515.
[22] J.-P. Fouassier, J. Lalevée, Photoinitiators for Polymer Synthesis-scope, Reactivity, and Efficiency, Wiley-VCH Verlag GmbH & Co.KGaA, Weinheim, 2012.
[23] W.F. Schroeder, S.V. Asmussen, M. Sangermano, C.I. Vallo, Visible light polymerization of epoxy monomers using an iodonium salt with camphorquinone/ethyl-4-dimethyl aminobenzoate, Polym. Int. 24 (2013) 430.
[24] S.V. Asmussen, I.E. delÍErba, W.F. Schroeder, C.I. Vallo, Photopolymerization of methacrylate monomers using polyhedral silsesquioxanes bearing side-chain amines as photoinitiator, Eur. Polym. J. 48 (2012) 309.
[25] S. Kumar-Krishnan, E. Prokhorov, M. Hernández-Iturriaga, J.D. Mota-Morales, M. Vázquez-Lepe, Y. Kovalenko, I.C. Sanchez, G. Luna-Bárcenas, Chitosan/silver nanocomposites: synergistic antibacterial action of silver nanoparticles and silver ions, Eur. Polym. J. 67 (2015) 242.
[26] K.K. Wong, X. Liu, Silver nanoparticles – the real "silver bullet" in clinical medicine?, Med Chem. Commun. 1 (2010) 125.
[27] J.P. Phillips, N.M. Mackey, B.S. Confait, D.T. Heaps, X. Deng, M.L. Todd, S. Stevenson, H. Zhou, C.E. Hoyle, Dispersion of gold nanoparticles in UV-cured, thiol-ene films by precomplexation of gold-thiol, Chem. Mater. 20 (2008) 5240.
[28] G. Carotenuto, M. Palomba, A. Longo, S. De Nicola, L. Nicolais, Optical limiters based on silver nanoparticles embedded in amorphous polystyrene, Sci. Eng. Compos. Mater. 18 (2011) 187.
[29] O.D. McNair, B.J. Sparks, A.P. Janisse, D.P. Brent, D.L. Patton, D.A. Savin, Highly tunable thio-ene networks via dual thiol addition, Macromolecules 46 (2013) 5614.
[30] C.I. Vallo, Influence of filler content on static properties of glass-reinforced bone cement, J. Biomed. Mater. Res. Appl. Biomater. 53 (2000) 717.